Oncogene (2008) 27, 5339–5347

www.nature.com/onc

ORIGINAL ARTICLE

Interaction of folliculin (Birt-Hogg-Dubé gene product) with a novel Fnip1-like (FnipL/Fnip2) protein

Y Takagi[1,2], T Kobayashi[1], M Shiono[1], L Wang[1], X Piao[1], G Sun[1], D Zhang[1], M Abe[1], Y Hagiwara[1,3], K Takahashi[2] and O Hino[1]

[1]*Department of Pathology and Oncology, Juntendo University School of Medicine, Bunkyo-Ku, Tokyo, Japan;* [2]*Respiratory Medicine, Juntendo University School of Medicine, Bunkyo-Ku, Tokyo, Japan and* [3]*Division of Manufacturing, Research and Development, Immuno-Biological Laboratories Co. Ltd, Fujioka-shi, Gunma, Japan*

Birt-Hogg-Dubé (BHD) syndrome is characterized by the development of pneumothorax, hair folliculomas and renal tumors and the responsible *BHD* gene is thought to be a tumor suppressor. The function of folliculin (Flcn), encoded by *BHD*, is totally unknown, although its interaction with Fnip1 has been reported. In this study, we identified a novel protein binding to Flcn, which is highly homologous to Fnip1, and which we named FnipL (recently reported in an independent study as Fnip2). The interaction between FnipL/Fnip2 and Flcn may be mediated mainly by the C-terminal domains of each protein as is the case for the Flcn-Fnip1 interaction. FnipL/Fnip2 and Flcn were located together in the cytoplasm in a reticular pattern, although solely expressed Flcn was found mainly in the nucleus. Cytoplasmic retention of Flcn was canceled with C-terminal truncation of FnipL/Fnip2, suggesting that FnipL/Fnip2 regulates Flcn distribution through their complex formation. By the employment of siRNA, we observed a decrease in S6K1 phosphorylation in the *BHD*-suppressed cell. We also observed a decrease in S6K1 phosphorylation in *FNIP1*- and, to a lesser extent, in *FNIPL*/*FNIP2*-suppressed cells. These results suggest that Flcn-FnipL/Fnip2 and Flcn-Fnip1 complexes positively regulate S6K1 phosphorylation and that FnipL/Fnip2 provides an important clue to elucidating the function of Flcn and the pathogenesis of BHD.
Oncogene (2008) **27,** 5339–5347; doi:10.1038/onc.2008.261; published online 28 July 2008

Keywords: *BHD*; S6K1; AMPK; FnipL/Fnip2; Fnip1

Introduction

Birt-Hogg-Dubé (BHD) syndrome is an autosomal dominantly inherited disease characterized by the development of pneumothorax, hair folliculomas and renal tumors (Birt *et al*., 1977). In 2002, Nickerson *et al*. (2002) identified the predisposing gene of BHD (*BHD*) by positional cloning strategy (Schmidt *et al*., 2001). The *BHD* gene is located on chromosome 17p11.2 and encodes folliculin (Flcn), an evolutionary conserved protein (~67 kDa) with no apparent functional motif (Nickerson *et al*., 2002). From the observations of a second somatic inactivation, *BHD* is thought to be a tumor suppressor (Vocke *et al*., 2005).

We have studied the mechanism of multistep carcinogenesis using animal models of hereditary renal carcinoma (RC), such as the Eker rat and the Nihon rat (Hino *et al*., 2003). The Eker rat has a germline alteration in the homolog of human *TSC2* (*Tsc2*), a predisposing gene of the tuberous sclerosis complex (Kobayashi *et al*., 1995). The Nihon rat has been characterized by earlier development and more aggressive phenotypes of RCs relative to the Eker rat (Okimoto *et al*., 2000). Heterozygous Nihon mutant rats develop RCs that mainly show clear-cell histology. Homozygous mutants are embryonic lethal in both Eker and Nihon rats (Okimoto *et al*., 2004a). In 2004, we identified a germline mutation in the rat homolog of *BHD* (*Bhd*) (Okimoto *et al*., 2004b). Subsequently, we demonstrated a suppression of the Nihon rat's phenotypes by transgenic introduction of a wild-type *Bhd* mini-gene (Togashi *et al*., 2006). Thus the Nihon rat became an animal model of BHD (Kouchi *et al*., 2006). There is also a dog model available of BHD, which has a missense mutation in the *Bhd* homolog (Lingaas *et al*., 2003).

To better understand the molecular mechanism of *BHD*/*Bhd* mutation-associated pathogenesis, the elucidation of Flcn's function is necessary. However, besides its tumor suppressive role, little is known about the physiological activity of Flcn. In a study using *Drosophila*, involvement of the *Bhd* homolog in the JAK-STAT and Dpp pathways was expected from the results of RNA interference (RNAi) experiments (Singh *et al*., 2006). Baba *et al*. (2006) identified a novel, evolutionally conserved, human Flcn-binding protein (Fnip1). They demonstrated that the Fnip1 protein also interacts with the AMPK complex and that both Flcn and Fnip1 are phosphorylated by AMPK (Baba *et al*., 2006). They also reported that the phosphorylation of

Correspondence: Dr O Hino, Department of Pathology and Oncology, Juntendo University School of Medicine, 2-1-1 Hongo, Bunkyo-Ku, Tokyo 113-8421, Japan.
E-mail: ohino@juntendo.ac.jp
Received 24 January 2008; revised 2 June 2008; accepted 30 June 2008; published online 28 July 2008

Flcn is regulated directly or indirectly by mTOR and that the phosphorylation of S6K1 might be modulated by Flcn expression under certain circumstances (Baba *et al*., 2006). Interestingly, a recent report using mutants of the *Bhd* homolog in fission yeast demonstrated that *Bhd*-deficiency causes downregulation of Tor2 (van Slegtenhorst *et al*., 2007). Conversely, in fission yeast, *Drosophila* and mammals, a deficiency of *Tsc2* homolog activates the rapamycin-sensitive Tor/mTOR pathway (Guertin and Sabatini, 2007; van Slegtenhorst *et al*., 2007). These findings suggest that the mTOR pathway in different ways may be involved in various pathogenesis.

Although the mTOR pathway must be important in the pathogenesis of BHD syndrome, it may not be the sole signal transduction system associated with Flcn. We are exploring the function of Flcn by using *in vivo* (Nihon rats) as well as *in vitro* experimental systems (Kouchi *et al*., 2006; Togashi *et al*., 2006). In this study, we report the identification and characterization of a novel Flcn-binding protein, FnipL (for Fnip1-Like), which is highly homologous to Fnip1. During the course of the review process of this report, the same Flcn-binding protein was reported as Fnip2 by another group (Hasumi *et al*., 2008).

Results

Identification and expression of an FNIP1-*related gene,* FNIPL

In a database search, we noticed the presence of a human gene, *KIAA1450* that is highly homologous to *FNIP1*. *KIAA1450* was originally identified in a cDNA-sequencing project carried out by the Kazusa DNA Research Institute (Nagase *et al*., 2000). *KIAA1450* is localized on human chromosome 4q, whereas *FNIP1* is on chromosome 5q (HUGE data base, Kazasa DNA Research Institute; http://www.kazusa.or.jp/huge/) (Nagase *et al*., 2001). Comparison of deduced amino-acid sequences revealed that *KIAA1450* had a putative initiation codon and a subsequent sequence similar to those of the amino-terminal region of the Fnip1 product (Figure 1). Therefore, *KIAA1450* was thought to cover the full-coding region. The product of KIAA1450 consisted of 1114 amino-acid residues and showed 49.1% sequence identity with human Fnip1 (DQ145719; 1166 residues), through its entire length (Figure 1 and data not shown). In FnipL, there were sequences corresponding to the evolutionary conserved five blocks previously found among Fnip1 orthologs (Figure 1) (Baba *et al*., 2006). In addition to these five blocks, several other conserved blocks between KIAA1450 and Fnip1 were found (data not shown). From these similarities, we designated *KIAA1450* as *FNIPL* (*FNIP1-like*) in this study. So far, we have found *FNIPL* orthologs in various mammals and avians, but not in other vertebrates or the invertebrates, *Caenorhabditis elegans* and *Drosophila melanogaster* (data not shown).

Expressions of *FNIPL*, *FNIP1* and *BHD* in human tissues were examined by Northern blot analysis using gene-specific probes. As shown in Figure 2, *FNIPL* showed an expression profile that was relatively similar to those of *FNIP1* and *BHD*. The strongest expression of *FNIPL* mRNA was observed in the heart with two different bands (7.5 and 6.5 kb). The molecular basis for generating these two bands is currently unknown. A high expression of *FNIPL* mRNA was also found in placenta and liver, and moderate expression was found in lung, small intestine, kidney and brain. The similarity of expression profiles among those genes suggests that the FnipL and Flcn as well as Fnip1 are functionally related.

Binding of Flcn to FnipL

When N-terminal Myc-tagged full-length FnipL (Myc-FnipL) was expressed in Cos7 cells, it appeared

```
            Block1
hFnipL  134' DVNMLGEMMFGSVAMSYKGSTLKIHYIRSPPQLMISKVFSARMG 177
             *.********************** ********.****.** *
hFnip1  125" DANMLGEMMFGSVAMSYKGSTLKIHQIRSPPQLMLSKVFTARTG 168

            Block2
hFnipL  307' RKKKIAISIIFSLCEKEEAQRNFQDFFFSHFPLFESHMNRLKSAIEKAMISCRKIAESSLRVQFYVSRLMEALGEFRGTIWNLYSVPRIAEPVWLTMMS 405
             *.*****..****...*.....*.***************.******.**  .*. *..* *   * .*...**.***.** ***.***.*********
hFnip1  326" RKKKIAIGVIFSLSKDEDENNKFNEFFFSHFPLFESHMNKLKSAIEQAMKMSRRSADASQRSLAY-NRIVDALNEFRTTICNLYTMPRIGEPVWLTMMS 423

            Block3
hFnipL  433' FFAALLTAVLTYHLAWVPTVMPVDHPPIKAFSEKRTSQSVNMLAKTHPYNPLWAQLGDLYGAIGSPVRLTRTVVVGKQKDLVQRILYVLTYFLRCSELQENQLTWSGNHG 542
             *..**.***** ********** ..**** * **..****.*****************************.*******.*.***.** ****.*******..*   .* .
hFnip1  451" FLPALITAVLTNHLAWVPTVMPNGQPPIKIFLEKHSSQSVDMLAKTHPYNPLWAQLGDLYGAIGSPVRLARTVVVGKRQDMVQRLLYFLTYFIRCSELQETHL--LENGE 558

            Block4
hFnipL  972' QCLVADLVHTVHHPVLDEPIAEAVCIIADTDKWSVQVATSQRK 1014
             ***..** *.*.***************** ***.****.***.
hFnip1 1025" QCLMSDLSHAVQHPVLDEPIAEAVCIIADMDKWTVQVASSQRR 1067

            Block5
hFnipL 1021' LGQDVLVSSQVSSLLQSILQLYKLHLPADFCIMHLEDRLQEMYLKSKMLSEYLRGHTRVHVKELGVVLGIESNDLPLLTAIASTHSPYVAQILL 1114
             **.***** **.**.*.***** .*...**.*********.*.**********. **************.*****.*.************
hFnip1 1073" LGKEVLVSSLVSNLLHSTLQLYKHNLSPNFCVMHLEDRLQELYFKSKMLSEYLRGQMRVHVKELGVVLGIESSDLPLLAAVASTHSPYVAQILL 1166
```

Figure 1 Comparison of Fnip1 and FnipL sequences. Five evolutionary conserved sequence blocks (human) previously found in Fnip1 homologues are compared with the human FnipL sequence. Identical residues and conservative substitutions are indicated with asterisks and dots, respectively.

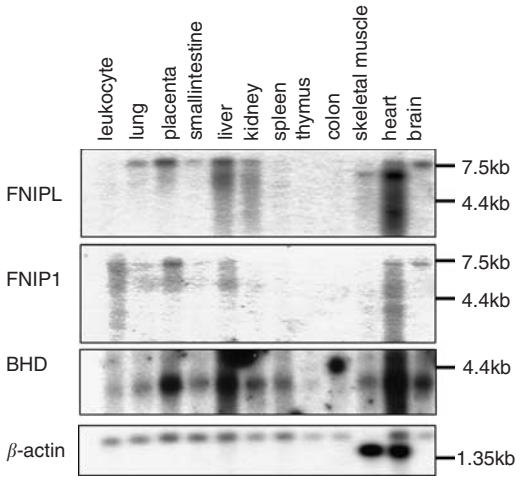

Figure 2 Expression of *FNIPL*, *FNIP1* and *BHD* mRNAs in human tissues. The indicated probes (left) were used for Northern blot analysis. Positions of size markers (KB) are shown on the right.

as an ~130-kDa protein by western blotting, which coincides with a calculated molecular weight of 122 kDa (Figure 3a). As reported previously, several bands of Flcn appeared by western blotting (Baba *et al*., 2006). To examine the interaction between Flcn and FnipL, we performed immunoprecipitations in Cos7 cells transiently expressing N-terminal Flag-tagged Flcn (Flag-Flcn) and Myc-FnipL. It was revealed that Flcn was coimmunoprecipitated with FnipL in a reciprocal manner, as in the case with Fnip1 (Figure 3b). We have not detected complex formation between Fnip1 and FnipL when they were coexpressed, suggesting that Fnip1 and FnipL independently interact with Flcn (data not shown). Next, we generated an FnipL-specific rabbit polyclonal antibody (Figure 3a). This antibody did not recognize Fnip1 when it was tested by immunoblotting using transiently expressed proteins. By using this FnipL-specific antibody and anti-Flcn antibody, endogenous Flcn-FnipL interaction in HEK293 cells was confirmed by reciprocal coimmunoprecipitations (Figure 3c). These results indicate that Flcn and FnipL physically interact with each other and that there are two complexes, Flcn-Fnip1 and Flcn-FnipL, *in vivo*.

Moreover, we noted that coexpression of Flcn with FnipL changes the behavior of Flcn bands on western blotting (Figure 3b). When the two proteins were coexpressed, the intensity of the slower migrating band of Flcn was increased. In the Flcn-FnipL immunocomplex, the slower migrating band was dominant, suggesting that FnipL binds more tightly to phosphorylated Flcn. These results are consistent with a reported case of Fnip1-Flcn interaction, as we confirmed in our analysis.

To identify the FnipL-binding domain, we used deletion mutants of Flcn lacking the N-terminal region (ΔSacI; 1–12 and 200–579 aa; Figure 3d, left panel) or C-terminal region (ΔC; 1–362 aa). Of these, only ΔSacI could be coimmunoprecipitated with FnipL after transient expression in Cos7 cells, suggesting that the FnipL-binding domain is present in the C-terminal region of Flcn (Figure 3d, left panel). Reciprocally, we examined the Flcn-binding domain in FnipL using its deletion mutants, such as ΔNspV (272–1114 aa), ΔEcoRI (381–1114 aa), ΔBstPI (544–1114) and ΔBglII (1–911 aa, Figure 3d, right panel). In the coimmunoprecipitation assay, only ΔBglII failed to interact with Flcn (Figure 3d, right panel). This suggests that the C-terminal region of FnipL is needed for binding to Flcn. Together, the interaction between Flcn and FnipL may be mediated mainly by their respective C-terminal domains, as in the case of Flcn-Fnip1 interaction (Baba *et al*., 2006).

Localization of FnipL and Flcn

We next analysed the distributions of FnipL, Flcn and Fnip1 by transient expression of epitope-tagged proteins in Cos7 cells. When expressed alone, Myc-FnipL was distributed in the cytoplasm (Figure 4a). It showed more condensed features around the nucleus. On the other hand, Flag-Flcn was found mainly in the nucleus when solely expressed (Figure 4a). However, when Myc-FnipL and Flag-Flcn were coexpressed they were located together in the cytoplasm in a reticular pattern. As reported previously, Myc-Fnip1 and Flag-Flcn were also located together in the cytoplasm (Figure 4b). These results demonstrate that FnipL, as well as Fnip1, regulates cytoplasmic distribution of Flcn. We next examined the endogenous distribution of these molecules by cellular fractionation analysis in HeLa cells (Figure 4d). FnipL and Fnip1 were enriched in the membrane fraction, although a small amount of the latter were found in other fractions. Flcn was also enriched in the membrane fraction, suggesting its colocalization with FnipL or Fnip1. The reticular pattern of Flcn/FnipL and Flcn/Fnip1 found in immunocytochemistry may reflect their association with some membranous components. Interestingly, a significant amount of Flcn was also found in the cytoskeletal fraction. This suggests that there are Flcn molecules free from FnipL- or Fnip1-binding in cells. In our analysis, histone H1 was found in the cytoskeletal fraction in addition to the nuclear fraction. Thus, it should not be excluded that the Flcn component found in the cytoskeletal fraction had been associated with nuclear components.

To ascertain whether the complex formation is necessary for FnipL-regulated cytoplasmic localization of Flcn, C-terminal-truncated FnipL (ΔBglII) was coexpressed with Flcn and their distributions were analysed. As shown in Figure 4, ΔBglII was still located in the perinuclear cytoplasm. However, cytoplasmic retention of Flcn was canceled with C-terminal truncation of FnipL, indicating that their colocalization in the cytoplasm is regulated through the complex formation.

Binding and phosphorylation of FnipL by AMPK

The AMPK complex was also reported as an Flcn-binding component (Baba *et al*., 2006). By means of transient expression and coimmunoprecipitation, we also detected an interaction of N-terminal HA-tagged

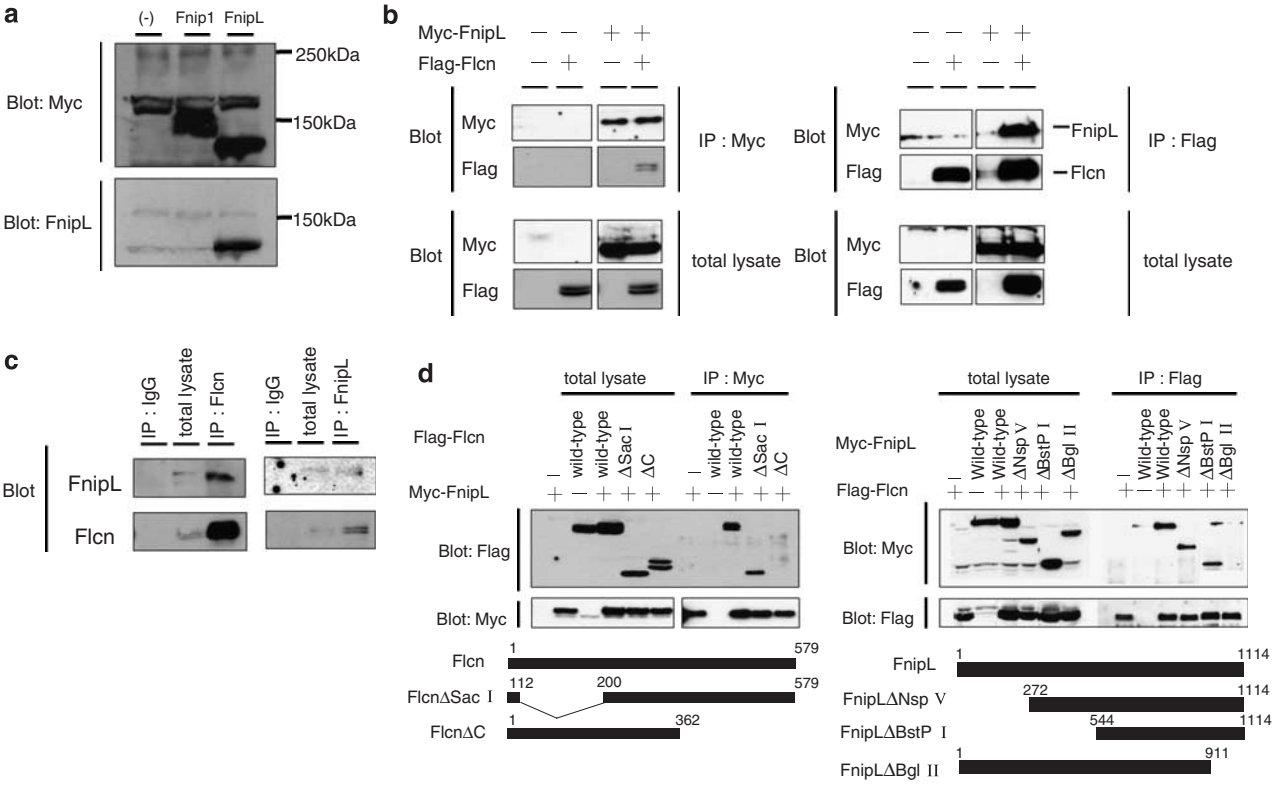

Figure 3 Interaction of FnipL with Flcn. (**a**) Western blot analysis of transiently expressed Myc-FnipL and Myc-Fnip1 in Cos7 cells. After transfection of plasmids, cells were lysed and protein samples were analysed by western blotting using anti-Myc antibody and anti-FnipL antibody. Lanes: (−), empty plasmid. Size markers (kDa) are indicated on the right. (**b**) Coimmunoprecipitation of Flcn and FnipL. Expression plasmids for Flag-Flcn, Myc-Fnip1 and Myc-FnipL were transfected into Cos7 cells by indicated combinations. Cells were lysed and lysates were immunoprecipitated with anti-Flag or anti-Myc antibodies. Immunocomplexes (IP: Myc and IP: Flag) as well as total lysates (total lysate) were analysed by western blotting. (**c**) Endogenous Flcn-FnipL interaction. HEK293 lysates were reciprocally coimmunoprecipitated with anti-Flcn or anti-FnipL and blotted with anti-FnipL or anti-Flcn. Normal rabbit IgG was used as a control antibody. (**d**) Deletion analysis of Flcn (right panel). Full-length (WT) or N-terminal- (ΔSacI) or C-terminal- (ΔC) deleted Flag-Flcn were transiently expressed with (+) or without (−) Myc-FnipL. Cell lysates (total lysate) and the immunocomplex obtained by anti-Myc antibody (IP: Myc) were analysed by western blotting using anti-Flag antibody. Deletion analysis of FnipL (left panel). Full-length (WT) or deletion mutant (ΔNspV, ΔBstP1 and ΔBglII) FnipL were transiently expressed with (+) or without (−) Flag-Flcn. Cell lysates (total lysate) and the immunocomplex obtained by anti-Flag antibody (IP: Flag) were analysed by western blotting using anti-Myc antibody.

FnipL with N-terminal Myc-tagged α1 subunit of AMPK (Figure 5). When coexpressed with FnipL, the amount of AMPK α1 subunit tended to increase. When the interaction of the AMPK α1 subunit and deletion mutants of FnipL were assessed, both ΔBstP1 and ΔBglII showed binding activity, suggesting that the AMPK-binding domain is located between 544–911 aa of FnipL (Figure 5). This region corresponds to the AMPK-binding region of Fnip1, between the evolutionary conserved domains 3 and 4, although the sequence homology is relatively low (data not shown). An *in vitro* kinase assay revealed that FnipL is phosphorylated by AMPK α1 subunit (Figure 5). Thus, FnipL may receive functional modulation from AMPK similarly to that received by Fnip1.

Suppression of S6K1 phosphorylation by BHD-, FNIPL- or FNIP1 knockdown

To explore the effects of *BHD*- as well as *FNIP1*- or *FNIPL* suppression, we employed RNAi experiments in HeLa cells in which those three genes were expressed. After transfection of siRNAs for *BHD*, knockdown was assessed by western blot analysis of Flcn and was found to be efficiently accomplished (~85% suppression compared with control cells using β-actin as a control) (Figure 6). As some relationship between Flcn and the mTOR pathway has been demonstrated, we analysed the phosphorylation of S6K1 (Thr389) and found that it was attenuated in the *BHD*-suppressed cells (mean ± s.d. = 0.71 ± 0.17 relative to control cells in phospho-S6K/S6K band ratio, $P = 0.04$) (Figure 6). Next, we examined the effects of *FNIP1* and *FNIPL* suppression (~85 and ~60% suppression, respectively, compared with control cells) (Figure 6). Intriguingly, we also observed a decrease of S6K1 phosphorylation in *FNIPL*- or *FNIP1*-suppressed cells (Figure 6). *FNIP1* suppression significantly reduced S6K1 phosphorylation (0.66 ± 0.09 relative to control cells, $P = 0.02$). *FNIPL* suppression also showed subtle reduction in the S6K1 phosphorylation (0.89 ± 0.03 relative to control cells, $P = 0.03$). Together, these analyses suggest that a

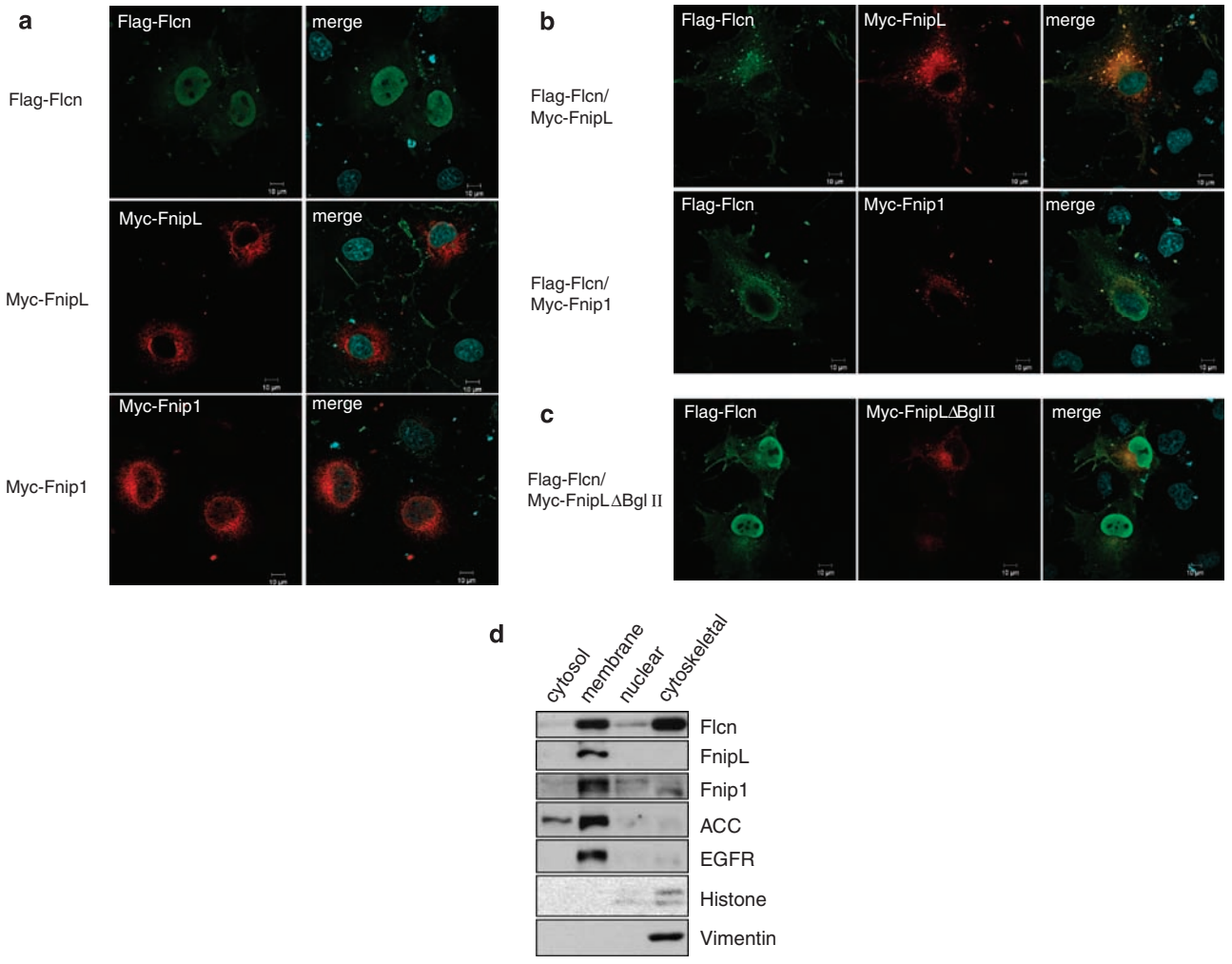

Figure 4 Localization of Flcn and FnipL. (**a**) Single expression of Flcn, FnipL and Fnip1. Flag-Flcn, Myc-FnipL or Myc-Fnip1 was transiently expressed alone in Cos7 cells. Immunocytochemistry was performed with anti-Flag or anti-Myc antibodies. DAPI was used for nuclear staining. (**b**) Colocalization of Flcn and FnipL. Cos7 cells were transiently expressed with Flag-Flcn and Myc-FnipL or Myc-Fnip1. (**c**) Effect of C-terminal deletion of FnipL on Flcn localization. C-terminal-truncated Myc-FnipL (ΔBglII) was coexpressed with full-length Flag-Flcn. (**d**) Cell fractionation analysis. Fractions of HeLa cell extract were analysed by western blotting for Flcn, FnipL and Fnip1. Acetyl CoA carboxylase (ACC, cytosolic and membrane), EGF receptor (EGFR, membrane), histone H1 (nuclear) and vimentin (cytoskeletal) were analysed as marker proteins for fractionation.

Flcn-FnipL or Flcn-Fnip1 complex positively regulates S6K1 phosphorylation. As an implication of the mTOR phosphorylation in the activation of mTOR∼S6K1 pathway has been suggested, we assessed the phosphorylation status of mTOR (Ser2448) in RNAi analysis. Unexpectedly, we observed a decrease in the total mTOR level after treatment with *BHD*, *FNIPL* or *FNIP1* siRNAs (Figure 6c). Accordingly, levels of phosphorylated mTOR (phospho-mTOR) were also decreased (Figure 6c). Effects of Flcn-FnipL and Flcn-Fnip1 complex on mTOR itself were predicted. However, differences in the level of total mTOR and phospho-mTOR were not similar to those of target molecules of RNAi (Figure 6 and data not shown). Although we could not conclude that Flcn modulates the S6K1 phosphorylation through regulation of mTOR phosphorylation, its function may directly or indirectly affect mTOR.

Discussion

Besides its role as a tumor suppressor, the function of the *BHD* gene is not clearly understood, but molecular characterization through the identification of binding proteins will provide functional information about Flcn. To approach a characterization of Flcn Baba *et al.* (2006) identified and studied Fnip1 , and in this study we have identified FnipL as a novel Flcn-binding protein. FnipL is highly homologous to Fnip1 in terms of primary structure as well as functional association with Flcn. As expected from the sequence conservation, FnipL binds to Flcn through its C-terminal domain. Our analysis revealed that the FnipL-binding domain is located in the C-terminal half of Flcn as is the Fnip1-binding domain. Although a detailed analysis is required, Fnip1 and FnipL may share the same domain of Flcn for binding. FnipL shows other properties

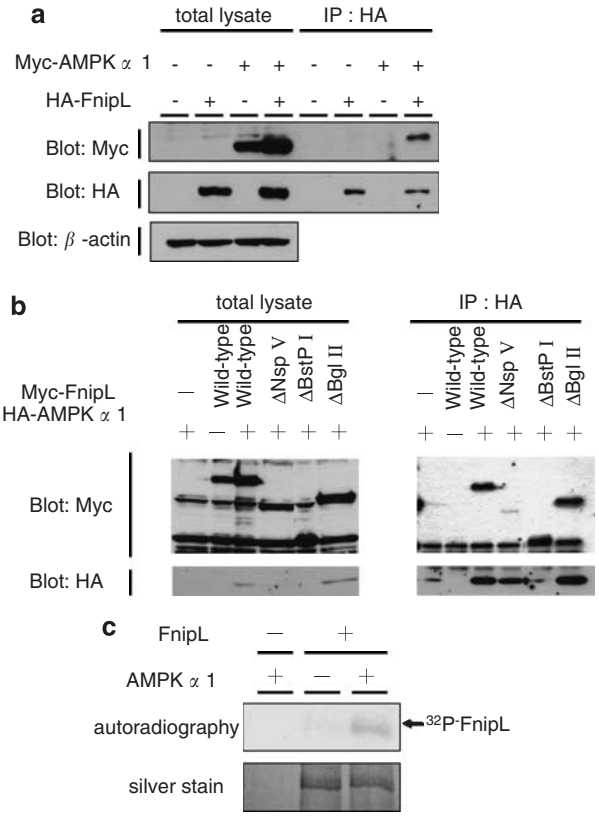

Figure 5 Binding and phosphorylation of FnipL by AMPK. (**a**) Complex formation of FnipL with AMPK. Expression plasmids for HA tagged FnipL and Myc-AMPKα1 were transfected into Cos7 cells in the indicated combinations. Total cell lysates (total lysate) were immunoprecipitated with anti-HA (IP) and analysed by western blotting with anti-Myc and anti-HA antibodies. ß-actin was used as a loading control. (**b**) Interactions of FnipL deletion mutants with AMPK. Full-length (WT) or deletion mutant (ΔNspV, ΔBstP1 or ΔBglII) FnipL were transiently expressed with HA-AMPKα1. Cell lysates (total lysate) and the immunocomplex obtained by precipitation with anti-HA antibody (IP: HA) were analysed by western blotting using anti-Myc or anti-HA antibody. (**c**) Phosphorylation of FnipL by AMPK. Flag-FnipL, synthesized by *in vitro* translation, was incubated with (+) or without (−) active AMPKα1 subunit in the presence of γ^{32}P-ATP. After SDS–PAGE, radioactivity was analysed by an image analyzer.

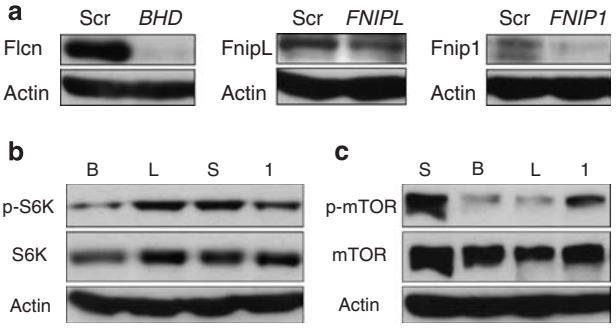

Figure 6 S6K1 and mTOR phosphorylation after *BHD*, *FNIPL* or *FNIP1* knockdown. (**a**) Suppression of target genes. HeLa cells were transfected with siRNAs for target genes (*BHD*, left; *FNIPL*, middle; *FNIP1*, right panel) or control dsRNA (Scr). After 48 h, lysates were analysed for western blotting with indicated antibodies. β-actin was used as a control (actin). (**b**) Analysis of S6K1 phosphorylation. Cell extracts obtained after siRNA treatment (48 h) were analysed by western blotting with antibodies for phospho-Thr389 S6K1 (p-S6K), S6K1 (S6K) or β-actin (actin). Lanes: B, *BHD* siRNA; L, *FNIPL* siRNA; S, control dsRNA; 1, *FNIP1* siRNA. (**c**) Analysis of mTOR phosphorylation. Western blotting was performed as in (**b**) with antibodies for phospho-Ser2448 mTOR (p-mTOR), mTOR or β-actin (actin).

similar to those of Fnip1. As previously reported for Fnip1, FnipL may positively regulate phosphorylation of Flcn, and it also binds efficiently to the phosphorylated form of Flcn. One possible role of FnipL may be to prevent dephosphorylation of Flcn through their complex formation. FnipL is bound and phosphorylated by AMPK. The phosphorylation of Flcn by AMPK was also reported previously (Baba *et al*., 2006). However, the roles that these phosphorylations play in the functions of Flcn, FnipL and Fnip1 are currently not understood.

In this study, we found that the siRNA-mediated suppression of Flcn expression in mammalian cells, at least in HeLa cells, results in the downregulation of S6K1 phosphorylation. Several recent studies have suggested some relationship between Flcn and the mTOR∼S6K1 pathway (Baba *et al*., 2006; van Slegtenhorst *et al*., 2007). Baba *et al*. (2006) reported a rapamycin-sensitive phosphorylation of Flcn, which suggests a direct or indirect involvement of mTOR in the regulation of Flcn function. They also reported an Flcn-dependent modulation of S6K1 phosphorylation under particular culture conditions . For example, during amino-acid starvation, the phosphorylation of S6K1 (Thr389) was suppressed in *BHD*-null cells but not in Fcln expression-reconstituted cells (Baba *et al*., 2006). On the contrary, the S6K1 phohsphorylation was retained under serum-starved condition in *BHD*-null cells but not in Flcn-reconstituted cells (Baba *et al*., 2006). Thus various culture conditions may affect the regulatory mechanism of mTOR∼S6K1 by Flcn. Although our analysis was performed under the amino-acid-sufficient condition, some stress condition during transfection procedure may contribute to the observed changes in S6K1 phosphorylation. More recently, a kidney-specific conditional knockout of mouse *Bhd* homolog was reported (Baba *et al*., 2008). It resulted in the polycyst formation and elevated mTOR function. In that study, the authors also suggested different responses of mTOR signals to *BHD* gene status between different experimental systems (Baba *et al*., 2008). Interestingly, fission yeast mutants of the *Bhd* homolog were more sensitive to rapamycin and resulted in downregulation of the Tor2 complex (TORC1) (van Slegtenhorst *et al*., 2007). In *Saccharomyces cerevisiae*, the LST7 product shows significant homology with Flcn (our unpublished observation), and *LST7* mutants exhibit somewhat similar phenotypes to those of *LST8*, the gene of a TORC1 component (Roberg *et al*., 1997). The products of the *TSC2* gene (tuberin) and its homologues function in the down-regulation of TORC1 (Guertin and Sabatini, 2007). Thus, at least under certain conditions, Flcn may have the opposite effect of tuberin in terms of mTOR

regulation in mammalian cells. As mTOR function is regulated by various signal transduction systems, cell type- or condition-specific role of Flcn on mTOR should not be excluded.

FNIP1 knockdown exerted a similar effect as *BHD* knockdown on the S6K1 phosphorylation. *FNIPL* knockdown induced only a subtle change in the S6K1 phosphorlylation. This might be owing to the incomplete suppression of *FNIPL* or to a lower contribution of FnipL than Fnip1 in the regulation of S6K1 phosphorylation. Two complexes, Flcn-FnipL and Flcn-Fnip1, may function independently in the mTOR regulation and that suppression of their common factor, Flcn, may cause severe effects than Fnip1 or FnipL suppression. Intriguingly, products of yeast *Bhd* homologs lack the region corresponding to the C-terminal half of mammalian Flcn, and there seems to be no yeast Fnip1 or FnipL homologs. Perhaps the regulation of the Flcn function by Fnip1 and FnipL play a modulatory role.

Very recently, FnipL has been identified in a similar homology-based approach and named Fnip2 (Hasumi *et al*., 2008). This latter report presented similar results on the Flcn-FnipL/Fnip2 interaction, however Hasumi *et al*. (2008) also found a binding between Fnip1 and FnipL/Fnip2, whereas we have not identified their strong interaction in forced expression experiments. This difference might be derived from the different experimental conditions and we cannot rule out binding between Fnip1 and FnipL/Fnip2.

So far, there are no identified differences between FnipL/Fnip2 and Fnip1 in their functional properties. However, the expression profiles of *FNIPL*/*FNIP2* and *FNIP1* mRNAs in human tissues are somewhat different because *FNIPL*/*FNIP2* exhibits higher expression in the liver. In addition, Hasumi *et al*. (2008) reported different expression profiles of *FNIP1* and *FNIPL*/*FNIP2* in renal cancers. The primary structures of Fnip1 and FnipL/Fnip2 are significantly different in the region between the evolutionary conserved domains 3 and 4 (Baba *et al*., 2006). This region may be a key to elucidate the functional differences between these two Flcn partners and the two different complexes that include Flcn. Functional differences between those two complexes may provide important clues to understanding the pathogenesis of BHD syndrome and other *BHD* mutation-associated diseases.

Materials and methods

Plasmid construction

For the transient expression in mammalian cells, the pCAG-GS expression vector was used (Niwa *et al*., 1991). N-terminal Flag-, HA- or Myc-tag coding sequence and appropriate multi-cloning sites were introduced using synthetic oligonucleotides. All PCRs and reverse-transcription (RT)-PCRs were carried out by using the Expand High Fidelity PCR System (Roche, Mannheim, Germany) and all subclones were confirmed by sequence analysis. Full-length human *BHD* cDNA was amplified from a HeLa cell cDNA pool using the primers HBHF1 (5′-CCGAATTCAATGC CATCGTGGCTCTCTG-3′) and HBHR1 (5′-CCCTCGAGT CAGTTCCGAGACTCCGAGG-3′) and subcloned after digestion with *Eco*RI and *Xho*I (at sites underlined in the primer sequences). A partial cDNA clone (KIAA1961) for the Fnip1-encoding gene (*FNIP1*) and full-length cDNA clone (KIAA1450) for the FnipL-encoding gene (*FNIPL*) were obtained from Kazusa DNA Research Institute (Kisarazu, Japan). The 5′-part of *FNIP1* cDNA was amplified using the primers HFPF11 (5′-GTCTCGAGCATGGCCCCTACG CTGTTCCA-3′) and HFPR11 (5′-TGGGTTAGGGCCAC AGCTTTCATC-3′) and used to construct a full-coding sequence after digestion with *Xho*I (underline) and *Hind*III (internal site). For KIAA1450 cDNA, the 5′-part of the coding sequence was modified by PCR amplification and re-cloned using the primers HFPF21 (5′-GGCTCGAGCATGGCCCC GACCCTGCTCCA-3′) and HFPR21 (5′-CCATACAGGTT CAGCTATCCTTGG-3′) after digestion with *Xho*I (underline) and *Eco*RI (internal site). Full-length cDNAs for S6K1 and AMPKα1 subunit were amplified from a rat embryonic cDNA pool using the following primers: S6KF1 (5′-CGGAATTCG CAGGAGTGTTTGACATAGAC-3′) and S6KR1 (5′-CG GGTACCTCATAGATTCATACGCAGGTG-3′) for S6K1; AMPKF1 (5′-CGGAATTCGCCGAGAAGCAGAAGCAC GA-3′) and AMPKR1 (5′-GGAGATCTTTACTGTGCAA GAATTTTAATTAGAT-3′) for AMPKα1. Amplified cDNAs were subcloned after digestion with restriction enzymes (sites are underlined in primer sequences). Expression plasmids for deletion mutants of Flcn (ΔSacI and ΔC) and FnipL (ΔNspV, ΔBstPI and ΔBglII) were constructed by using appropriate restriction sites as indicated in results (see below in Figure 3). Details of deletion are available upon request.

For *in vitro* translation, the full-length cDNA for N-terminal Flag-tagged FnipL was amplified using primers HFNIPLF1 (5′-ATGGACTACAAGGATGACGATGACAAGGCCCCG ACCCTGCTCCA-3′) and HFNIPLR1 (5′-GGGGTACCAA GGAAGAACTGTCCTGAGC-3′) and subcloned into the pTD1 vector (Shimadzu, Kyoto, Japan).

Northern blot analysis

For northern blotting, *FNIPL* and *FNIP1* cDNA fragments showing lowest homology were used as probes. Briefly, a *FNIPL* cDNA was amplified by PCR from the constructed plasmid using primers FNOF2 (5′-CCGAATTCCCAGCAT CAGACGCTTCCT-3′) and FNOR2 (5′-TGGACACGACCT CGGACAACTTAAGGG-3′), subcloned and then used as a probe. Similarly, a *FNIP1* cDNA was generated from the constructed plasmid cDNA using primers FNOF1 (5′-GGG AATTCTTGCAGTCATCCACTCCTTG-3′) and FNOR1 (5′-AAGGAGTCGTCCTGGTTTCTCTTAAGCC-3′. For *BHD*, the full-length cDNA was used as a probe. Northern blotting was performed by using a human multiple tissue northern blot membrane (Clontech, Mountain View, CA, USA).

Cell culture and plasmid transfection

Cos7, HeLa and HEK293 cells were cultured in Dulbecco's modified Eagle's medium (DMEM; Sigma, St Louis, MO, USA) supplemented with 10% FCS in humidified 5% CO_2 at 37 °C. Plasmids were transfected into Cos7 cells with Fugene 6 (Roche) according to the manufacturer's instructions. Cells were harvested after 48 h incubation. For siRNA transfection, see below (*RNAi* section).

Antibodies

Antibodies for phospho-Thr-389 S6K, phospho-Ser-2448 mTOR, mTOR and acetyl CoA carboxylase were purchased

from Cell Signaling Technology (Danvers, MA, USA). Antibodies for S6K (C19), EGF receptor (1005) were from Santa Cruz Biotechnology (Santa Cruz, CA, USA). Anti-vimentin (V9) and anti-histone H1 (AE4) antibodies were from Dako (Glostrup, Denmark) and Upstate (Lake Placid, NY, USA), respectively. Rabbit polyclonal antibodies for Flag (F7425), Myc (C3956), mouse monoclonal antibodies for Flag (M2), Myc (9E10) and β-actin (AC15) were from Sigma. A mouse monoclonal anti-HA (12CA5) antibody was from Roche. Anti-Flcn C1 antibody was reported previously (Okimoto *et al*., 2004b). Rabbit polyclonal anti-Flcn 223 antibody was generated against a synthetic peptide (CNTAFTPFLHQRNGNAARSL) corresponding to amino-acid residues (aa) 223–241 of human Flcn (IBL, Fujioka Japan). Rabbit polyclonal anti-Fnip1 655 and anti-FnipL 75 antibodies were generated by immunizing with the following peptides (IBL): Fnip1 655, CQEENAVDVKQYRDKLRT; FnipL 75, VTAQKTEDVPIKISAKC. All antibodies were affinity-purified and reciprocal cross-reactivities were checked by western blotting using transiently expressed proteins.

Immunoprecipitation and cell fractionation
Flag-Flcn, Myc-FnipL, Myc-Fnip1 and deletion mutants of Flcn and FnipL were transiently expressed in Cos7 cells. Cells were lysed on ice in NP40 lysis buffer (10 mM Tris-HCl pH 7.4, 150 mM NaCl, 0.5 mM EDTA, 10 mM NaF, 1% Nonidet P-40) with protease inhibitors (aprotinin, leupeptin, pepstatin A) and phosphatase inhibitors (1 mM Na_3VO_4, 10 mM β-glycerophosphate, 10 mM sodium pyrophosphate). The lysate was immunoprecipitated at 4 °C overnight with antibodies and protein G plus protein A agarose (Calbiochem, Darmstadt, Germany) or with anti-HA agarose (Sigma). The resin was washed three times with ice-cold phosphate-buffered saline and bound proteins were dissolved in SDS–PAGE gel loading buffer, followed by boiling and subjected to western blot analysis. Cell fractionation was performed using Fraction-PREP Cell Fractionation System (BioVision, Mountain View, CA, USA) according to the manufacturer's instructions.

Western blot analysis
Protein concentration was determined by the DC-protein assay (Bio-Rad, Hercules, CA, USA). Equal amounts of proteins were subjected to SDS–polyacrylamide gel electrophoresis, transferred to Immobilon-P membrane (Millipore, Billerica, MA, USA), blocked in 1% skim milk in Tris-buffered saline containing 0.05% Tween 20, and blotted with the appropriate antibodies**.** To probe with rabbit antibodies, Envision system (Dako) was used as described (Fukuda *et al*., 2000). To probe with mouse antibodies, anti-mouse immunoglobulin and streptavidin-biotinylated horseradish peroxidase (GE Healthcare, Buckinghamshire, UK) were used in second and third steps**,** respectively. For detection, ECL reagents (GE Healthcare) were used.

Immunocytochemistry
HeLa cells transfected with Myc-FnipL, Myc-FnipLΔBglII, Myc-Fnip1 and Flag-Flcn expression plasmids were cultured on a glass bottom dish (Matsunami, Osaka, Japan) for 48 h. Cells were washed with ice-cold phosphate-buffered saline and fixed with 2% paraformaldehyde and permeabilized with 0.1% Triton X-100 for 30 min at 4 °C. Incubation with anti-Flag (mouse) and anti-Myc (rabbit) antibodies was performed at 4 °C for 1 h in phosphate-buffered saline containing 0.05% Tween 20. The secondary antibodies used were Alexa Fluor 488-conjugated goat anti-mouse IgG and Alexa Fluor 568-conjugated goat anti-rabbit IgG (Invitrogen, Carlsbad, CA, USA). DAPI was used for counterstaining. After 1 h incubation with the secondary antibodies, cells were examined by using a laser-scanning microscope (LSM510 META; Zeiss, Thornwood, NY, USA).

In vitro *translation and* in vitro *kinase assay*
In vitro translation was performed by using T7 RiboMAX Express RNA production system (Promega, Madison, WI, USA) and Transdirect insect cell system (Shimadzu) according to the manufacturer's instructions. Flag-tagged FnipL was purified by affinity chromatography through anti-Flag (M2) agarose (Sigma) and was used as a substrate. For kinase assay, Flag-FnipL was incubated with or without recombinant GST-AMPKα1 (aa 1–312; Cell Signaling Technology) in a solution consisting of 60 mM HEPES-NaOH pH 7.5, 3 mM $MgCl_2$, 3 mM $MnCl_2$, 1 mM dithiothreitol, 5% polyethyleneglycol and 0.5 mM ATP (with 1 μCi/μl γ-^{32}P-ATP). The samples were separated by a 10% SDS–PAGE and then silver staining and autoradiography were performed.

RNAi
Transfection of siRNA into HeLa cells was performed with Lipofectamine 2000 (Invitrogen) at a final concentration of 40 nM according to the manufacturer's instructions. After 48 h cells were lysed with SDS–PAGE lysis buffer and analysed by western blotting. siRNA sequences used were as follows (sense and antisense in 5′–3′ orientation): for *BHD*, SIHB3 (GGUA CAGCAUCAUCACCAUTT and AUGGUGAUGAUGCU GUACCTT); for *FNIPL*, HFLS1 (GCCUGAUCUUGUG CUUCAUTT and AUGAAGCACAAGAUCAGGCTT); for *FNIP1*, HFP1S1 (CCCUGUGAACUUCCCUGUUTT and AACAGGGAAGUUCACAGGGTT). Results of western blotting were analysed by using ImageJ software (ver. 1.39u). At least three independent experiments were utilized for quantitation and statistical analysis was performed using Student's *t*-test.

Acknowledgements

We thank Drs Fujii H, Tsurui H, Matsuoka S, Wakiya M, Kajino K, Mr Sasahara K and Mr Takagaki T in the Department of Pathology and Oncology for helpful discussions and technical supports. We also thank Ms Ochiai K and Mr Matsunami K in the Division of Radioisotope Research for expert support. We appreciate Dr Maeda M (IBL) for production of antibodies, and Drs Okimoto K, Matsumoto I and Kouchi M (Dainippon-Sumitomo Pharma) and Dr Maeda T (Tokyo University) for helpful discussions. We also thank Kazusa DNA Research Institute for cDNA clones. This study was supported by the grants from the Japan Society for the Promotion of Science (JSPS), from the Ministry of Education, Culture, Sports and Technology of Japan, and from the Ministry of Health, Labour and Welfare of Japan.

References

Baba M, Furihata M, Hong SB, Tessarollo L, Haines DC, Southon E *et al*. (2008). Kidney-targeted Birt-Hogg-Dubé gene inactivation in a mouse model: Erk1/2 and Akt-mTOR activation, cell hyperproliferation, and polycystic kidneys. *J Natl Cancer Inst* **100**: 140–154.

Baba M, Hong SB, Sharma N, Warren MB, Nickerson ML, Iwamatsu A *et al*. (2006). Folliculin encoded by the *BHD* gene interacts with a binding protein, FNIP1, and AMPK, and is involved in AMPK and mTOR signaling. *Proc Natl Acad Sci USA* **103**: 15552–15557.

Birt AR, Hogg GR, Dube WJ. (1977). Hereditary multiple fibrofolliculomas with trichodiscomas and acrochordons. *Arch Dermatol* **113**: 1674–1677.

Fukuda T, Tani Y, Kobayashi T, Hirayama Y, Hino O. (2000). A new western blotting method using polymer immunocomplexes: Detection of Tsc1 and Tsc2 expression in various cultured cell lines. *Anal Biochem* **285**: 274–276.

Guertin DA, Sabatini DM. (2007). Defining the role of mTOR in cancer. *Cancer Cell* **12**: 9–22.

Hasumi H, Baba M, Hong SB, Hasumi Y, Huang Y, Yao M *et al*. (2008). Identification and characterization of a novel folliculin-interacting protein FNIP2. *Gene* **415**: 60–67.

Hino O, Kobayashi T, Momose S, Kikuchi Y, Adachi H, Okimoto K. (2003). Renal carcinogenesis: genotype, phenotype and dramatype. *Cancer Sci* **94**: 142–147.

Kobayashi T, Hirayama Y, Kobayashi E, Kubo Y, Hino O. (1995). A germline insertion in the tuberous sclerosis (*Tsc2*) gene gives rise to the eker rat model of dominantly inherited cancer. *Nat Genet* **9**: 70–74.

Kouchi M, Okimoto K, Matsumoto I, Tanaka K, Yasuba M, Hino O. (2006). Natural history of the Nihon (Bhd gene mutant) rat, a novel model for human Birt-Hogg-Dubé syndrome. *Virchows Arch* **448**: 463–471.

Lingaas F, Comstock KE, Kirkness EF, Sorensen A, Aarskaug T, Hitte C *et al*. (2003). A mutation in the canine *BHD* gene is associated with hereditary multifocal renal cystadenocarcinoma and nodular dermatofibrosis in the German shepherd dog. *Hum Mol Genet* **12**: 3043–3053.

Nagase T, Kikuno R, Ishikawa K, Hirosawa M, Ohara O. (2000). Prediction of the coding sequences of unidentified human genes. XVII. The complete sequences of 100 new cDNA clones from brain, which code for large proteins *in vitro*. *DNA Res* **7**: 143–150.

Nagase T, Kikuno R, Ohara O. (2001). Prediction of the coding sequences of unidentified human genes. XXII. The complete sequences of 50 new cDNA clones which code for large proteins. *DNA Res* **8**: 319–327.

Nickerson ML, Warren MB, Toro JR, Matrosova V, Glenn G, Turner ML *et al*. (2002). Mutations in a novel gene lead to kidney tumors, lung wall defects, and benign tumors of the hair follicle in patients with the Birt-Hogg-Dubé syndrome. *Cancer Cell* **2**: 157–164.

Niwa H, Yamamura K, Miyazaki J. (1991). Efficient selection for high-expression transfectants with a novel eukaryotic vector. *Gene* **108**: 193–199.

Okimoto K, Kouchi M, Kikawa E, Toyosawa K, Koujitani T, Tanaka K *et al*. (2000). A novel 'Nihon' rat model of a mendelian dominantly inherited renal cell carcinoma. *Jpn J Cancer Res* **91**: 1096–1099.

Okimoto K, Kouchi M, Matsumoto I, Sakurai J, Kobayashi T, Hino O. (2004a). Natural history of the Nihon rat model of BHD. *Curr Mol Med* **4**: 887–893.

Okimoto K, Sakurai J, Kobayashi T, Mitani H, Hirayama Y, Nickerson ML *et al*. (2004b). A germ-line insertion in the Birt-Hogg-Dubé (*BHD*) gene gives rise to the Nihon rat model of inherited renal cancer. *Proc Natl Acad Sci USA* **101**: 2023–2027.

Roberg KJ, Bickel S, Rowley N, Kaiser CA. (1997). Control of amino acid permease sorting in the late secretory pathway of Saccharomyces cerevisiae by SEC13, LST4, LST7 and LST8. *Genetics* **147**: 1569–1584.

Schmidt LS, Warren MB, Nickerson ML, Weirich G, Matrosova V, Toro JR *et al*. (2001). Birt-Hogg-Dubé syndrome, a genodermatosis associated with spontaneous pneumothorax and kidney neoplasia, maps to chromosome 17p11.2. *Am J Hum Genet* **69**: 876–882.

Singh SR, Zhen W, Zheng Z, Wang H, Oh SW, Liu W *et al*. (2006). The Drosophila homolog of the human tumor suppressor gene BHD interacts with the JAK-STAT and dpp signaling pathways in regulating male germline stem cell maintenance. *Oncogene* **25**: 5933–5941.

Togashi Y, Kobayashi T, Momose S, Ueda M, Okimoto K, Hino O. (2006). Transgenic rescue from embryonic lethality and renal carcinogenesis in the Nihon rat model by introduction of a wild-type *Bhd* gene. *Oncogene* **25**: 2885–2889.

van Slegtenhorst M, Khabibullin D, Hartman TR, Nicolas E, Kruger WD, Henske EP. (2007). The Birt-Hogg-Dubé and tuberous sclerosis complex homologs have opposing roles in amino acid homeostasis in Schizosaccharomyces pombe. *J Biol Chem* **282**: 24583–24590.

Vocke CD, Yang Y, Pavlovich CP, Schmidt LS, Nickerson ML, Torres-Cabala CA *et al*. (2005). High frequency of somatic frameshift *BHD* gene mutations in birt-hogg-dube-associated renal tumors. *J Natl Cancer Inst* **97**: 931–935.